Continuous-time Analog Computing Circuits for Solving The Electromagnetic Wave Equation

Nilan Udayanga, Arjuna Madanayake, S.I. Hariharan, and Nathaniel Hawk
The University of Akron, Ohio, USA.
{gnu1,arjuna,hari,nah38}@uakron.edu

***Abstract*—Two continuous-time mathematical computing methods are proposed for solving the multidimensional wave equation leading to realizable analog computing circuits. The proposed analog computing processors will potentially be able to solve a certain special classes of computational problems involving partial differential equations, which are defined from continuous-time systems. The new analog computing methods are first derived and physically implemented for the first-time using low-frequency operational amplifier circuits in order to experimentally verify the correctness of the proposed methods. Both algorithms approximate the spatial domain partial derivatives using discrete finite differences. The first method performs a direct Laplace transform (with respect to the time variable) on the resulting expression. The second method applies the finite difference along the time dimension and then replaces the discrete time difference with a continuous-time delay operator, which in turn, can be realized as an analog all-pass filter. Analog circuit architectures are introduced for different boundary conditions relevant to common electromagnetic simulation problems. A low frequency prototype of the analog wave equation solver (based on method 1) has been designed, realized and tested using board-level operational amplifier circuits. Test results and measurements are provided to demonstrate the wave propagation in the space-time domain.**

I. Introduction

Analog computing can accelerate certain special classes of computational problems involving partial differential equations (PDEs) defined from continuous-time systems [1]–[11]. Most physics based simulations involve either linear or non-linear PDE systems. Electromagnetics, which is an extremely important branch of physics, is completely described by Maxwell's equations, which are in turn, first order linear PDEs [12]–[14]. Therefore, there has been immense efforts in the computational electromagnetics community to simulate electromagnetic models by first descretizing the Maxwell's equations using a staggered computational grid and then solving by digital computers using software [15]–[19]. However, Maxwell's equations are themselves time-continuous, and therefore allow a natural fit for linear analog computing systems using simulation models based on spatially-discrete-time-continuous update equations. We demonstrate the concept by proposing a simplified analog computer that solves the spatio-temporal wave-equation using an analog array processor that operates in continuous-time mode. We have developed two methods producing mathematical models, one of which has been realized using analog circuits. A low-frequency implementation based on operational amplifiers (op-amps) is used to demonstrate the new analog algorithms, with RF extension part of on-going work not covered in this paper.

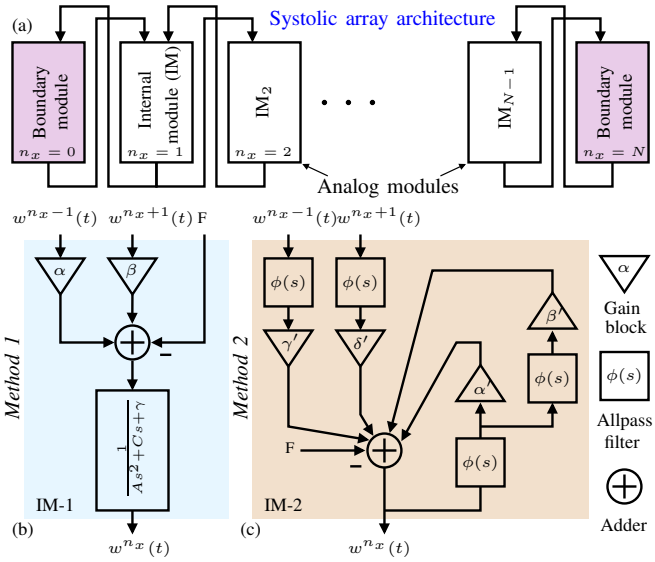

Fig. 1: Systolic array architecture of the second order continuous-time PDE solver. Block diagram of the internal module (IM) derived from (b) *method 1* and (c) *method 2*.

In the first method, partial derivatives in the spatial dimension are approximated using discrete finite differences, while applying Laplace transformation (LT) for partial derivatives in the time dimension [20], [21]. This results in a mixed domain (spatially-discrete and time-continuous) transfer function leading to a continuous-time (analog) implementation of the PDE solver. The second method starts with the finite difference time domain (FDTD) method (Yee algorithm). The finite differences in time are replaced with a continuous-time delay operator (of duration τ), which can be realized efficiently on analog RF CMOS technology as an active-circuit based analog all-pass filter [22], [23]. Both methods introduced are based on a general two dimensional (2-D) second order PDE. The governing PDE of the 1-D wave equation (one spatial dimension and time dimension) is used to verify the proposed methods. A low-frequency prototype of the proposed spatially-discrete-time-continuous wave equation solver (based on *method 1*) is designed, simulated and realized using discrete analog integrated circuits (ICs) and surface mount components.

In order to derive mathematical models and discover corresponding analog circuits to solve linear PDEs, consider a 2-D constant coefficient second order linear PDE in the form of

978-1-5386-4881-0/18/$31.00 ©2018 IEEE

$$A\frac{\partial^2 w(x,t)}{\partial t^2}+B\frac{\partial^2 w(x,t)}{\partial x^2}+C\frac{\partial w(x,t)}{\partial t} + D\frac{\partial w(x,t)}{\partial x}+Ew(x,t)+F=0, \tag{1}$$

where x $(0<x<L)$ and t $(0<t)$ are the spatial and time variables, respectively (A, B, C, D, E, and F are constants). $x=0$ and $x=L$ correspond to the left and right boundaries, respectively. $w(x,t)$ is a solution of the PDE.

II. Method 1: Direct Laplace Transform Method

As the first step, approximate the spatial domain partial derivatives using the finite difference approximations (with a grid spacing of Δx) [24]. Spatial discretization of the resulting expression leads to

$$A\frac{\partial^2 w^{n_x}(t)}{\partial t^2}+B\left[\frac{w^{n_x+1}(t)-2w^{n_x}(t)+w^{n_x-1}(t)}{\Delta x^2}\right] + C\frac{\partial w^{n_x}(t)}{\partial t}+D\left[\frac{w^{n_x}(t)-w^{n_x-1}(t)}{\Delta x}\right] + Ew^{n_x}(t)+F=0, \tag{2}$$

where the superscript of the function $w^{n_x}(t)$ denotes the spatial index ($n_x \in \{0,1,2,\ldots,N\}$). Here, $n_x=0$ and $n_x=N$ correspond to the spatial locations at the left and right boundaries ($\Delta x = L/N$). The first and second order derivatives are approximated using the backward (with first order accuracy) and central (with second order accuracy) differences, respectively. The most suitable finite difference method (forward, backward or central) can be selected based on the resulting mathematical model (select the one which leads to a realizable analog circuit with the lowest hardware complexity). The second step is to apply the LT along the time dimension. The resulting mixed domain expression is

$$As^2W^{n_x}(s)+\frac{B}{\Delta x^2}\left[W^{n_x+1}(s)-2W^{n_x}(s)+W^{n_x-1}(s)\right] + CsW^{n_x}(s)+\frac{D}{\Delta x}\left[W^{n_x}(s)-W^{n_x-1}(s)\right] + EW^{n_x}(s)+F=0. \tag{3}$$

Zero initial conditions are considered for the LT. The spatially-discrete-time-continuous expression for the n_x^{th} spatial location can then be obtained as

$$W^{n_x}(s)=\frac{\alpha W^{n_x-1}(s)+\beta W^{n_x+1}(s)-F}{As^2+Cs+\gamma}, \tag{4}$$

where, $\alpha=-\frac{B}{\Delta x^2}+\frac{D}{\Delta x}$, $\beta=\frac{-B}{\Delta x^2}$, and $\gamma=-\frac{2B}{\Delta x^2}+\frac{D}{\Delta x}+E$. This expression can be used to implement the internal analog module, which computes the solution to the internal spatial locations (i.e. $n_x \in \{1,2,\ldots,N-1\}$). The internal module (IM) that computes the solution $w^{n_x}(t)$ (at the n_x^{th} spatial location) requires $w^{n_x-1}(t)$ and $w^{n_x+1}(t)$ functions as the inputs, which correspond to the solutions at n_x-1 and n_x+1 spatial locations, respectively. The numerator polynomial $\alpha W^{n_x-1}(s)+\beta W^{n_x+1}(s)-F$ can be realized using operational amplifiers (scaling and summing), where as the $\frac{1}{As^2+Cs+\gamma}$ operator can be implemented using a passive LRC circuit or an active circuit realization method (e.g. Sallen-Key topology [25]). The continuous-time solution to the PDE given in (1) can be obtain by connecting each modules in a systolic array architecture as shown in Fig. 1 (a). Fig. 1 (b) shows the corresponding IM. The proposed method can be extended to multiple dimensions and higher order PDEs.

At each boundary ($n_x=0$ and $n_x=N$), different modules need to be implemented based on the governing equations at the boundary. The Dirichlet boundary condition specifies the solution $w^0(t)$ at the boundary. Thus, we do not need any additional hardware to implement the boundary module. A signal source that produces the corresponding solution $w^0(t)$ can be used to excite the IM at $n_x=1$ (i.e. the $w^{n_x-1}(t)$ input of the IM_1 is $w^0(t)$). The initial conditions at the left boundary are defined by $w^0(t)$. The Neumann boundary $\left.\frac{\partial w(x,t)}{\partial x}\right|_{x=N\Delta x}=0$ can be realized by connecting the $w^{n_x+1}(t)$ input to the $w^{n_x-1}(t)$ input of the IM at the boundary [since $w^{N+1}(t)=w^{N-1}(t)$].

III. Method 2: All-pass Filter Based Method

The second continuous-time method for solving MD PDEs is proposed based on a direct mapping from digital domain FDTD implementations to the continuous-time analog architectures. Analog models are realized by replacing unit sample delays in a digital prototype with an all-pass analog filter, thereby converting a digital prototype to a continuous-time analog version. As the first step, apply the central finite difference on (2) with respect to t, while keeping the time variable continuous. This leads to

$$Kw^{n_x}(t)=\alpha' w^{n_x}(t-\tau)+\beta' w^{n_x}(t-2\tau) + \gamma' w^{n_x-1}(t-\tau)+\delta' w^{n_x+1}(t-\tau)-F, \tag{5}$$

where τ is the sample time delay, $\alpha'=\frac{2A}{\tau^2}+\frac{2B}{\Delta x^2\tau}-\frac{D}{\Delta x}-E$, $\beta'=\frac{-A}{\tau^2}+\frac{C}{2\tau}$, $\gamma'=\frac{-B}{\Delta x^2}+\frac{D}{\Delta x}$, $\delta'=\frac{-B}{\Delta x^2}$, and $K=\frac{A}{\tau^2}+\frac{C}{2\tau}$. Application of the LT on (5) with respect to the time variable t leads to a mixed domain expression (step 2)

$$KW^{n_x}(s)=\alpha' W^{n_x}(s)e^{-s\tau}+\beta' W^{n_x}(s)e^{-2s\tau} + \gamma' W^{n_x-1}(s)e^{-s\tau}+\delta' W^{n_x+1}(s)e^{-s\tau}-F. \tag{6}$$

Laplace domain representation $e^{-s\tau}$ is approximated as $e^{-s\tau}\approx\left[\frac{1-\frac{s\tau}{2m}}{1+\frac{s\tau}{2m}}\right]^m$, and can be realized in an analog RC-active topology using a cascade of m all-pass filters. Typically, $m=3$ is sufficient for approximation of τ [22]. Let $\phi(s)=\left(\frac{1-s\tau/2m}{1+s\tau/2m}\right)^m$ be the transfer function of all-pass filter that approximate the continuous-time delay τ. Fig. 1 (c) shows the block diagram of the proposed IM, where the all-pass filter $\phi(s)$ is used as a building block. Summing and scaling operations can be implemented using op-amp circuits. Note that this procedure is equivalent to a direct mapping from the digital FDTD implementation, where we replace the unit time delays with all-pass filters. Modules which correspond to each boundaries can be obtained by modeling the governing equations using the same method.

978-1-5386-4881-0/18/$31.00 ©2018 IEEE

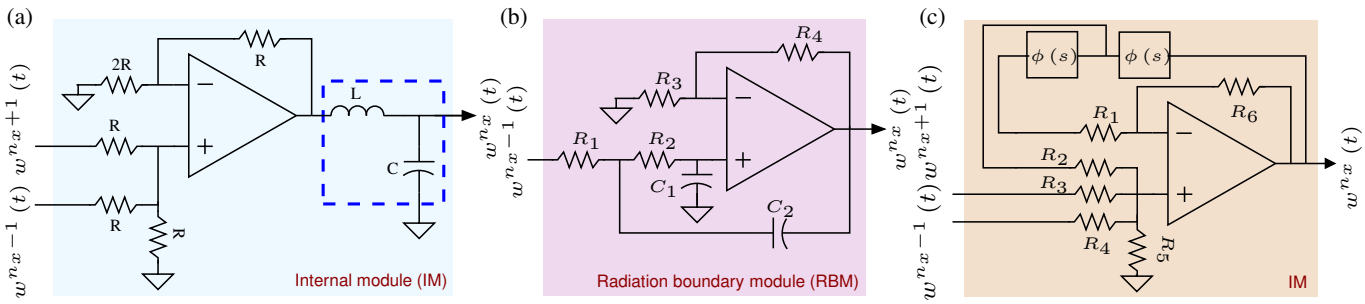

Fig. 2: Analog circuits for realizing (a) the internal module and (b) the boundary module for solving the continuous-time wave equation (using *method 1*) (c) Analog architecture of the internal module for the allpass filter based method (*method 2*).

IV. Analog Computing Circuits for Solving The Wave Equation

Proposed methods are utilized to find the continuous-time solution to the wave equation. Suppose that the function $w(x,t)$ provides the field intensity of a wave at position x and time t. Then, $w(x,t)$ satisfies the PDE [26], [27]

$$\frac{1}{c^2}\frac{\partial^2 w(x,t)}{\partial t^2} = \frac{\partial^2 w(x,t)}{\partial x^2}, \tag{7}$$

where c is the velocity of the signal. Application of *method 1* leads to the following mixed domain expression

$$W^{n_x}(s) = \frac{W^{n_x+1}(s) + W^{n_x-1}(s)}{2(As^2+1)}, \tag{8}$$

where $A \equiv \frac{\Delta x^2}{2c^2}$. The central difference is used to approximate the spatial derivative. The $\frac{1}{As^2+1}$ operation can be implemented using a series connection of an inductor (with value L) and a capacitor (with value C), where the output is obtained across the capacitor (see Fig. 2 (a)). Then the value A can be selected as $A = LC$. Alternatively, the Sallen-Key technique or the Bruton transformation can be used towards an active circuit realization. Scaling and summing operations can be realized using op-amp circuits. Fig. 2 (a) shows the analog circuit architecture corresponding to (8), which eventually solves the 1-D wave equation for internal spatial locations ($n_x = 1, 2, ..., N-1$). Radiation boundary condition at the right boundary ($n_x = N$) can be expressed as [26], [27]

$$\frac{1}{c}\frac{\partial w(x,t)}{\partial t}|_{x=N\Delta x} + \frac{\partial w(x,t)}{\partial x}|_{x=N\Delta x} = 0. \tag{9}$$

Application of *method 1* on (9) leads to $W^{N+1}(s) = W^{N-1}(s) - 2\frac{\Delta x}{c}sW^N(s)$. Thus, the mixed domain expression at $n_x = N$ can be obtained as (by substituting in (8))

$$W^N(s) = \frac{2W^{N-1}(s)}{\left(\frac{\Delta x}{c}\right)^2 s^2 + 2\frac{\Delta x}{c}s + 2}. \tag{10}$$

The radiation boundary module (RBM) can then be implemented using a LRC circuit (passive) or the Sallen-Key architecture (active) shown in Fig. 2 (b).

Application of *method 2* to find the continuous-time solution to the wave equation given in (7) leads to the following mixed domain expression, which can then be used to realize the corresponding IM ($K = \frac{\Delta x}{c\tau}$),

$$\begin{aligned} K^2 W^{n_x}(s) &= W^{n_x+1}(s)e^{-\tau s} + W^{n_x-1}(s)e^{-\tau s} \\ &+ 2\left(K^2-1\right)W^{n_x}(s)e^{-\tau s} - K^2 W^{n_x}(s)e^{-2\tau s}. \end{aligned} \tag{11}$$

Laplace domain representation $e^{-s\tau}$ is approximated using all-pass filters with a group delay of τ. The analog circuit architecture that computes the solution for internal spatial locations is shown in Fig. 2(c). The mixed domain expression for the radiation boundary at the right boundary is

$$\begin{aligned} K(K+1)W^N(s) &= 2\left(K^2-1\right)W^N(s)e^{-\tau s} \\ &+ K(1-K)W^N(s)e^{-2\tau s} + 2W^{N-1}(s)e^{-\tau s}, \end{aligned} \tag{12}$$

which can be realized as an architecture similar to the IM.

V. Analog Wave Equation Solver

The mathematical models that we developed in the previous sections were extended to an analog circuit implementation. Using *method 1*, we have designed, simulated and realized a low frequency prototype of the analog wave equation solver using op-amp ICs and surface mount components. The Bruton transformation has been employed to implement the passive LC circuit, mainly because of the difficulties in realizing high quality factor inductors at low frequencies [28], [29]. This will introduce a circuit element called frequency dependent negative resistance (FDNR) to the system, which can be realized using active circuits (op-amps). We have utilized the AD8056 op-amp IC for the design, which uses the standard voltage-feedback topology and has a 300 MHz of -3 dB bandwidth. The maximum operating frequency F_{max} is selected as 250 kHz (minimum wavelength $\lambda_{min} = \frac{c}{F_{max}}$). The distance between two spatial points Δx is set to be $\frac{\lambda_{min}}{2}$. Thus, the value A of the LC passive circuit [in (8)] is selected as $A = \frac{1}{8F_{max}^2} = 2 \times 10^{-12}$.

The Bruton transformation involves a impedance scaling of the circuit elements. All impedances $Z(s)$ in the circuit are transformed to $Z(s)/s$. The impedance transformation does not affect the voltage and current transfer and provides the original transfer function after the transformation. Thus, the passive LC circuit of the IM can be replaced by a circuit with a resistor and an FDNR element. The FDNR has a steady state impedance of $Z(s) = \frac{1}{-D\omega^2}$ [28]. Here, D is the value of the FDNR element. Such a circuit can be designed using the

978-1-5386-4881-0/18/$31.00 ©2018 IEEE

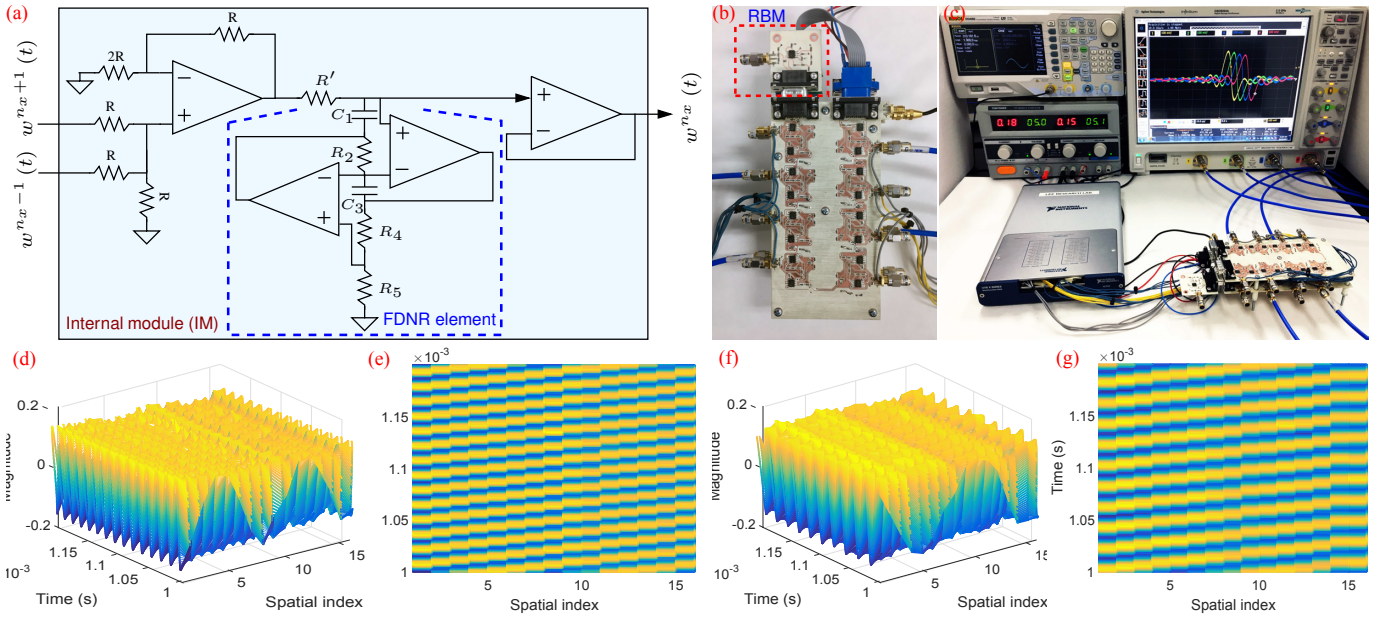

Fig. 3: (a) FDNR element based implementation of the internal module of the low frequency 1-D wave equation solver. (b) Interconnected 16-element analog wave equation solver. (c) Experiment setup to collect data. Obtained experiment results: Left boundary is excited using a sinusoidal signal with a center frequency of (d-e) 70 kHz and (f-g) 50 kHz (3-D and top views).

general impedance converter (GIC) method [28], [29]. By substituting capacitors and resistors at appropriate locations of the GIC, different types of impedances can be synthesized. The active circuit implementation of the FDNR element is shown in Fig. 3(a). Here, $D = \frac{C_1 R_2 C_3 R_4}{R_5}$. C_1 and C_3 capacitor values are selected as 10 nF. Resistor values $R_2 = 100\ \Omega$, $R_4 = 100\ \Omega$ and $R_5 = 50\ \Omega$ are used to obtain the appropriate A value. Output of the IM is buffered prior to feeding the adjacent elements. Thus, four op-amps are required to realize the IM. The RBM was implemented using the Sallen-Key architecture as shown in Fig. 2(b), which eventually solves Eq. (10). The S-domain transfer function of the circuit is [25]

$$H(s) = \frac{\frac{R_3+R_4}{R_3}}{R_1 R_2 C_1 C_2 s^2 + \left(R_1 C_1 + R_2 C_1 + R_1 C_2 \left(-\frac{R_4}{R_3}\right)\right) s + 1}.$$

Resistors and capacitors are selected as $R_1 = R_3 = R_4 = 100\ \Omega$, $R_2 = 200\ \Omega$, and $C_1 = C_2 = 10$ nF.

Eight- and sixteen-spatial location analog wave equation solvers have been realized using Rogers 4003C laminates and surface mount components. Eight internal modules were patterned on a single PCB. An RS232 connection was used so that multiple 8-spatial point boards could be easily connected together to form a longer chain. DC voltages are supplied to the boards through the RS232 connection. SMA connectors are used to capture the solution of each spatial location. Fig. 3 (b) shows the 16 spatial location analog wave equation solver along with the RBM board (top view). Data is captured using the national instrument data acquisition unit (sampling rate: 500 ksps). Fig. 3 (c) shows the experiment setup (4 outputs are shown in the oscilloscope when the left boundary is excited using a Gaussian pulse). Measured data are shown in Figs. 3 (d-g). The left boundary is excited using sinusoidal signals with a center frequency of 70 kHz (Fig.3(d-e)) and 50 kHz (Fig.3(f-g)). The right boundary is realized as a radiation boundary. The results clearly show the wave propagation in the space-time domain (with a constant velocity) and the effect of the radiation boundary (reflection free).

VI. Conclusion

Analog circuits have been proposed to compute the continuous-time solution of the wave equation. Two method have been introduced to map a given PDE to a corresponding analog circuit that can compute the solution to the PDE. The first method approximate the spatial domain partial derivatives with the finite differences while applying Laplace transformation along the time dimension. Corresponding analog circuits can be realized using op-amps and passive or active filters. The second method approximate both time and spatial domain derivatives with finite differences followed by replacing the time difference operations with continuous-time delay operators, which can be realized using all-pass filters. Both methods have been employed to derive analog circuits to design a continuous-time 1-D wave equation solver. A low frequency prototype of the proposed analog architecture (based on *method 1*) has been designed based on the Bruton transformation, Sallen-Key topology and FDNR elements. The designed system is realized using discrete ICs and surface mount components. Measured data is provided for a system where the left boundary is excited using a sinusoidal source, while the right boundary is realized as a radiation boundary.

Acknowledgment

The research is supported in part by national science foundation (NSF) 1629903 and defense advanced research projects agency (DARPA) D15C-002 via a subaward from Ocius Technologies.

978-1-5386-4881-0/18/$31.00 ©2018 IEEE

REFERENCES

[1] W. Little and A. Soudack, "On the analog computer solution of first-order partial differential equations," *Mathematics and Computers in Simulation*, vol. 7, no. 4, pp. 190 – 194, 1965. [Online]. Available: http://www.sciencedirect.com/science/article/pii/S0378475465800350

[2] L. D. K. Ach and W. Comley, "The analog computer as a teaching aid in diffential equations," *Mathematics and Computers in Simulation*, vol. 3, no. 2, pp. 60 – 63, 1961. [Online]. Available: http://www.sciencedirect.com/science/article/pii/S0378475461800244

[3] P.-A. Absil, "Continuous-time systems that solve computational problems." *IJUC*, vol. 2, no. 4, pp. 291–304, 2006.

[4] O. Bournez and M. L. Campagnolo, "A survey on continuous time computations," in *New Computational Paradigms*. Springer, 2008, pp. 383–423.

[5] G. E. R. Cowan, R. C. Melville, and Y. P. Tsividis, "A VLSI analog computer/math co-processor for a digital computer," in *IEEE International Solid-State Circuits Conference, Digest of Technical Papers.* IEEE, 2005, pp. 82–586.

[6] S. Fifer, *Analogue computation: theory, techniques, and applications*. McGraw-Hill, 1961, vol. 4.

[7] Y. Huang, N. Guo, M. Seok, Y. Tsividis, K. Mandli, and S. Sethumadhavan, "Hybrid analog-digital solution of nonlinear partial differential equations," in *Proceedings of the 50th Annual IEEE/ACM International Symposium on Microarchitecture*. ACM, 2017, pp. 665–678.

[8] N. Guo, Y. Huang, T. Mai, S. Patil, C. Cao, M. Seok, S. Sethumadhavan, and Y. Tsividis, "Energy-efficient hybrid analog/digital approximate computation in continuous time," *IEEE Journal of Solid-State Circuits*, vol. 51, no. 7, pp. 1514–1524, 2016.

[9] "Could analog computing accelerate complex computer simulations?" 2015. [Online]. Available: http://www.kurzweilai.net/could-analog-computing-accelerate-complex-computer-simulations

[10] Y. Huang, N. Guo, M. Seok, Y. Tsividis, and S. Sethumadhavan, "Evaluation of an analog accelerator for linear algebra," in *2016 ACM/IEEE 43rd Annual International Symposium on Computer Architecture (ISCA)*, June 2016, pp. 570–582.

[11] N. Guo, Y. Huang, T. Mai, S. Patil, C. Cao, M. Seok, S. Sethumadhavan, and Y. Tsividis, "Continuous-time hybrid computation with programmable nonlinearities," in *41st European Solid-State Circuits Conference (ESSCIRC)*, Sept 2015, pp. 279–282.

[12] M. Sadiku, *Elements of electromagnetics*. Oxford university press, 2014. [Online]. Available: http://www.ebook.de/de/product/21893771/matthew_sadiku_elements_of_electromagnetics.html

[13] M. F. Iskander, *Electromagnetic fields and waves*. Waveland Press, 2013.

[14] W. Chew, "150 years of maxwell's equations: A reflection," in *USNC-URSI Radio Science Meeting (Joint with AP-S Symposium)*. IEEE, 2014, pp. 288–288.

[15] W. C. Chew, E. Michielssen, J. Song, and J.-M. Jin, *Fast and efficient algorithms in computational electromagnetics*. Artech House, Inc., 2001.

[16] J.-M. Jin, *The finite element method in electromagnetics*. John Wiley & Sons, 2015. [Online]. Available: http://www.ebook.de/de/product/21080358/jian_ming_jin_the_finite_element_method_in_electromagnetics.html

[17] A. F. Peterson, S. L. Ray, R. Mittra, I. of Electrical, and E. Engineers, *Computational methods for electromagnetics*. IEEE press New York, 1998.

[18] G. Mur, "Absorbing boundary conditions for the finite-difference approximation of the time-domain electromagnetic-field equations," *IEEE transactions on Electromagnetic Compatibility*, no. 4, pp. 377–382, 1981.

[19] K. S. Kunz and R. J. Luebbers, *The finite difference time domain method for electromagnetics*. CRC press, 1993.

[20] L. T. Bruton, A. Madanayake, C. Wijenayake, and M. Maini, "Continuous-time analog two-dimensional IIR beam filters," *IEEE Transactions on Circuits and Systems II: Express Briefs*, vol. 59, pp. 419 –423, July 2012.

[21] N. Udayanga, A. Madanayake, and S. I. Hariharan, "Continuous-time algorithms for solving the electromagnetic wave equation in analog ICs," in *2017 IEEE 60th International Midwest Symposium on Circuits and Systems (MWSCAS)*, Aug 2017, pp. 29–32.

[22] C. Wijenayake, A. Madanayake, Y. Xu, L. Belostotski, and L. T. Bruton, "A steerable DC-1 GHz all-pass filter-sum RF space-time 2-D beam filter in 65 nm CMOS," in *2013 IEEE International Symposium on Circuits and Systems (ISCAS2013)*, May 2013, pp. 1276–1279.

[23] P. Ahmadi, B. Maundy, A. S. Elwakil, L. Belostotski, and A. Madanayake, "A new second-order all-pass filter in 130-nm CMOS," *IEEE Transactions on Circuits and Systems II: Express Briefs*, vol. 63, no. 3, pp. 249–253, March 2016.

[24] U. S. Inan and R. A. Marshall, *Numerical Electromagnetics: The FDTD Method*. Cambridge University Press, 2011. [Online]. Available: http://www.ebook.de/de/product/13945546/umran_s_stanford_university_california_inan_robert_a_stanford_university_california_marshall_numerical_electromagnetics.html

[25] R. P. Sallen and E. L. Key, "A practical method of designing RC active filters," *IRE Transactions on Circuit Theory*, vol. 2, no. 1, pp. 74–85, March 1955.

[26] C. H. Papas, *Theory of electromagnetic wave propagation*. Courier Corporation, 2014.

[27] W.-C. Wang, *Electromagnetic wave theory*. Wiley, New York, 1986.

[28] L. Bruton, "Network transfer functions using the concept of frequency-dependent negative resistance," *IEEE Transactions on Circuit Theory*, vol. 16, no. 3, pp. 406–408, Aug 1969.

[29] L. T. Bruton, *RC active circuits: theory and design*. Prentice hall, 1980.

978-1-5386-4881-0/18/$31.00 ©2018 IEEE